

Mechanical properties and structure of carotid arteries in mice lacking desmin

Patrick Lacolley^{a,*}, Pascal Challande^b, Saliha Boumaza^a, Géraldine Cohuet^a, Stéphane Laurent^a,
Pierre Boutouyrie^a, Jean-Alexis Grimaud^c, Denise Paulin^d, Jean-Marie Daniel Lamazière^c,
Zhenlin Li^d

^aInstitut National de la Santé et de la Recherche Médicale, INSERM U337, 15 Rue de l'École de Médecine, 75270 Paris Cedex 06, France

^bLMP CNRS-ESA 7068, Université Paris VI, 2 Place de la Gare de Ceinture, 78210 Saint-Cry l'École, France

^cLIP-CNRS-UMR 7623, Université Paris VI, 15 Rue de l'École de Médecine, 75270 Paris Cedex 06, France

^dMolecular Biology of Differentiation, Université Paris VII, 2 Place Jussieu, 75251 Paris Cedex 05, France

^eINSERM U441, Avenue du Haut-Lévêque, 33600 Pessac, France

Received 15 September 2000; accepted 1 March 2001

Abstract

Objective: Our aim was to determine in desmin homozygous mutant mice the viscoelastic properties, the mechanical strength and the structure of the carotid artery. **Methods:** To assess the viscoelastic properties of large arteries, we have performed an in vivo analysis of the diameter–, and distensibility–pressure curves of the common carotid artery (CCA) in homozygous (Des –/–), heterozygous (Des +/-) and wild-type (Des +/+) mice. To evaluate the mechanical strength, we have measured the in vitro intraluminal pressure producing the rupture of the carotid artery wall. The structure analysis of the arterial wall was based on histology and electronic microscopy. **Results:** A lower distensibility and an increase of arterial wall viscosity were observed in Des –/– compared with Des +/+. Arterial thickness of Des –/– was similar to those of Des +/+, without changes in elastin and collagen contents. Electron microscopy revealed that the perimeter of cellular fingerlike-projections was smaller in Des –/–, indicating that the cells have lost part of their connections to the extracellular matrix. The rupture pressure was significantly lower in Des –/– (1500±200 mmHg) compared with Des +/+ (2100±80 mmHg) indicating a lower mechanical strength of the vascular wall. No significant difference was found between Des +/- and Des +/+. **Conclusion:** The desmin is essential to maintain proper viscoelastic properties, structure and mechanical strength of the vascular wall. © 2001 Elsevier Science B.V. All rights reserved.

Keywords: Arteries; Extracellular matrix; Mechanotransduction; Smooth muscle; Ultrasound

1. Introduction

Desmin is the main component of the intermediate filaments in cardiac, skeletal and visceral smooth muscles [1]. To better analyze the role of desmin in vivo, two groups have generated mice deficient in desmin (Des –/–) by gene targeting [2,3]. These studies show that Des –/– mice are viable and fertile but have a very high mortality rate before the age of 1 year, mainly due to a severe cardiomyopathy [4]. The morphogenesis of the

striated [5] and smooth muscles [3] appears normal. However, important structural and ultrastructural defects are observed in the three types of muscles (i.e. increase in cell fragility and degeneration of muscle fibers). These alterations were prominent in very active muscles that are highly solicited, indicating that desmin is essential for integrity of myofibrils and cohesion of the muscles upon stress [3,5].

In vascular smooth muscle, desmin is associated with dense bodies and membrane-associated dense bands closely linked to actin filaments [6–8]. The function of desmin is not completely understood. It appears that desmin might

*Corresponding author. Tel.: +33-1-4407-9038; fax: +33-1-4407-9040.

E-mail address: lacolley@ccr.jussieu.fr (P. Lacolley).

Time for primary review 24 days.

provide an efficacious interaction between the cytoskeleton and the contractile elements to maintain the mechanical integrity of the vascular smooth muscle cells (SMC) [9,10].

In arteries, the functional consequences of the lack of desmin on stiffness and strength are not known. The only published study concerns visceral smooth muscles and shows a reduction in vitro of the contractile force [11]. Arterial function has not been studied yet, although vascular wall structure is abnormal in Des $-/-$ [2,3,10]. The main features are SMC disorganization, cellular hypoplasia, and loss of adhesion, which predominates in the thoracic aorta, particularly exposed to mechanical stress and, thus affected by the effects of fatigue.

To assess the viscoelastic properties of large arteries, we have performed an in vivo analysis of the diameter- and distensibility–pressure curves of the common carotid artery (CCA) in Des $-/-$, heterozygous mice (Des $+/-$) and wild-type (Des $+/+$) mice. To evaluate the mechanical strength, we have measured the in vitro intraluminal pressure producing the rupture of the carotid artery wall. This functional approach was coupled to a structural analysis with quantification of the main components of the arterial wall.

2. Methods

2.1. Animals

A null mutation in the desmin gene was introduced in the germ line of C57BL/6J as described by Li et al. [2]. Twenty-nine adult 3-month-old Des $-/-$ and 16 3-month-old Des $+/-$ were used in the experiments together with 26 age- and weight-matched wild-type mice. All procedures were in accordance with institutional guidelines for animal experimentation.

2.2. In vivo arterial mechanical parameters

We simultaneously recorded arterial diameter (left CCA) and blood pressure (right CCA), in pentobarbital anaesthetized mice, and determined arterial distensibility as previously described [12–15]. Arterial diameter was measured with an ultrasonic echo-tracking device (NIUS-01, Asulab SA, Neuchâtel, Switzerland). The relationship between the pressure P and the lumen cross-sectional area (LCSA) was fitted with the model of Langewouters et al. using an arctangent function and three optimal fit parameters (α , β and γ) [16]:

$$\text{LCSA} = \frac{\pi D^2}{4} = \alpha \left(\frac{\pi}{2} + \tan^{-1} \left(\frac{P - \beta}{\gamma} \right) \right) \quad (1)$$

where D is the internal diameter. Local arterial cross-

sectional distensibility $\text{Dist}(P)$ is defined by the relative change in LCSA for a given change in intravascular P :

$$\text{Dist}(P) = \frac{1}{\text{LCSA}} \times \frac{\delta \text{LCSA}}{\delta P}. \quad (2)$$

The arterial wall viscosity (AWV) is pointed out by the hysteresis of the pressure–LCSA curve which represents the fraction of energy dissipated within the wall. As previously described [17,18], AWV is expressed as the following ratio:

$$\text{AWV} = \frac{\text{WV}}{\text{WT}} \quad (3)$$

where WV is the dissipated viscous energy and WT the whole energy exchanged during one cardiac cycle. These values were averaged on about 20 cardiac cycles recorded during 4 s.

The calculation of hysteresis was made after the temporal resynchronization of the feet of pressure and diameter waves [17,18]. The pressure measurement was made by using a catheter (0.5 cm of PE-10 fused to 3 cm of PE-50; Clay Adams, Parsippany, NJ). Its use produced a residual underestimation of the hysteresis of about 0.6% which was taken into account in the computation of the in vivo hysteresis. The required synchronization has been achieved in nine Des $-/-$ and eight Des $+/+$.

2.3. Desmin expression and Western blot of cellular proteins

Total RNA from carotid arteries and aorta of mice was reverse transcribed into cDNA using MMLV Reverse Transcriptase and Oligo (dT)₁₇ primer. PCR reaction was processed by denaturation (94°C for 4 min) followed by 25 cycles: denaturation (1 min at 94°C), annealing (1 min at 62°C) and elongation (1 min at 72°C). PCR products were analyzed by electrophoresis on a 2% agarose gel, followed by ethidium bromide staining. The oligonucleotides used in PCR are as follows: for desmin gene, Desf 5'-AC-TCCCTGATGAGGCAGAT-3' and Desr 5'-GCTGAC-AACCTCTCCATCCCG-3'; for vimentin gene: Vimf 5'-GATTTCTCTGCCTCTGCCAAC-3' and Vimr 5'-GTGATGCTGAGAAGTCTCAT-3'. Primers were designed such that the amplified sequence spanned introns in order to exclude the genomic DNA contamination.

For desmin immunohistologic staining, 5- μm thick freeze-dried paraffin-embedded sections [14,19,20] or cryosections were used. Cryosections and freeze-dried tissue of CCA and thoracic aorta were fixed in acetone for 10 min. We performed the indirect immunoperoxidase technique with Tyramide signal amplification (NEN Life Science Products). Briefly, samples were treated with a peroxidase labeled mouse anti-desmin antibody (mAb) (Clone D33, DAKO). After three extensive washes in TBS, the biotinyl tyramide is added. After three washes in

TBS, the slides were again incubated with streptavidine–peroxidase complex. The presence of peroxidase was revealed after incubation with aminoethyl carbazole. The following controls were performed using omission of the first or second antibody.

A Western blot analysis of smooth muscle myosin heavy chain (SM-MHC) SM1 and SM2, nonmuscle-MHC (NM-MHC), α -actinin, vinculin and focal adhesion kinase (FAK) was performed following standard techniques. Arterial tissue was extracted from the carotid artery of Des $-/-$ ($n=6$) and Des $+/+$ ($n=6$). Total protein content was determined by the Bradford technique. Equal amounts (50 μ g) of the denatured proteins were loaded per lane, separated on a 4–15% SDS polyacrylamide gel and transferred to a nitrocellulose membrane. Membranes were incubated with monoclonal antibodies directed against SM-MHC SM1 (MCA MH02, Yamasa Corp., diluted at 1:100 000), SM-MHC SM2 (MCA MH03, Yamasa Corp., 1:100 000), NM-MHC (MCA MH04, Yamasa Corp., 1:50 000), vinculin (HVIN-1, Sigma, 1:400), α -actinin (BM 75.2, Sigma, 1:100) or a polyclonal antibody against FAK p125 (sc558, Santa Cruz, 3 μ g/ml).

Subsequent analysis utilized an anti-mouse, an anti-goat or anti-rabbit IgG peroxidase complex, as a second antibody (dilutions 1:3000–1:5000), and chemiluminescence emitted from luminol oxidized by peroxidase as a detection method (ECL system, Amersham).

2.4. Histomorphometry

We determined the structure of the CCA in 4% formaldehyde-fixed arteries at each animal's mean AP to provide the tissue fixation closest to the physiological in situ state of the vessel. As previously described [14], sirius red was used for collagen staining, orcein for elastin, and hematoxylin after periodic acid oxidation for nucleus staining. Carotid wall thickness, medial cross-sectional area (MCSA) and composition were then determined by computer-directed color analysis (Quant'Image software, Talence, France).

2.5. Electron microscopy

The thoracic aortas (2 Des $-/-$, 1 Des $+/+$ and 1 Des $+/-$) were fixed with 2.5% glutaraldehyde in 0.1 M phosphate buffer, pH 7.4, for 2 h. Following post-fixation for 1 h at 4°C in 2% osmic acid and alcohol dehydration, the samples were embedded in Epon resin. Ultrathin sections were stained with uranyl acetate and lead citrate on an LKB 2168 ultra-stainer and observed in a Philips CM.10 electron microscope. For quantification, six photographic montages per mouse were realized. On each of them, the length of the cellular fingerlike projection was measured at equivalent mean cellular perimeter.

2.6. Mechanical strength

The mechanical strength of the intact CCA was characterized by determining the in vitro intraluminal pressure leading to the vascular wall rupture [21]. One centimetre of the vessel free of collaterals was carefully dissected from Des $-/-$ ($n=6$), Des $+/-$ ($n=4$) and Des $+/+$ ($n=6$) mice. The arterial segment placed in warm (37°C) Krebs buffer was cannulated on a specially designed device and adjusted to its in situ length. An increasing intraluminal static pressure was applied and continuously measured by a pressure transducer (UP4, Pioden, Kent, UK) until the rupture of the vascular wall was achieved. The ruptures were confirmed on en face preparations.

2.7. Statistical analysis

All values were averaged and expressed as mean \pm S.E.M. One-way analysis of variance was performed to compare the three groups of mice. A Bonferroni test was used for intergroup comparison. Differences were considered significant at values of $P < 0.05$. To compare diameter and distensibility at the same AP level, we calculated the area under the curve (AUC) of each diameter–pressure curve and distensibility–pressure curve for the pulse pressure range common to the three groups (72–92 mmHg). We then compared the mean \pm S.E.M. of AUC of Des $-/-$ and Des $+/-$ with that of Des $+/+$.

3. Results

3.1. In vivo arterial mechanics

At 14 weeks of age, the Des $-/-$ mice were lighter than Des $+/+$ mice. Systolic AP (SAP) and pulse pressure (PP) were significantly lower in Des $-/-$ than in Des $+/+$. Mean AP (MAP), diastolic AP (DAP) and heart rate (HR) were not significantly different between Des $-/-$ and Des $+/+$ (Table 1).

The curves are determined within the respective diastolo-systolic AP range of each group (60–92 mmHg for Des $-/-$ and 72–104 for Des $+/+$). Within the common range of AP (72–92 mmHg), the diameter–pressure curve in Des $-/-$ was not significantly different from that of Des $+/+$, indicating no changes in arterial diameter for a given level of AP (Fig. 1a). By contrast, the distensibility–pressure curve of Des $-/-$ was significantly shifted downward compared with that of Des $+/+$, indicating a lower distensibility in Des $-/-$ (Fig. 1b). The mean shift of distensibility of Des $-/-$ compared with Des $+/+$ was equal to 3.7×10^{-3} mmHg $^{-1}$. Table 1 shows that there was no significant difference between Des $+/-$ and Des $+/+$ mice.

Table 2 shows that the total energy exchanged during the cardiac cycle was not significantly different between

Table 1

In vivo mechanical parameters of the carotid artery in Des $-/-$, Des $+/+$ and Des $+/-$ mice^a

Parameters	Des $-/-$ (n=11)	Des $+/+$ (n=11)	Des $+/-$ (n=11)
Weight, g	24±0.8	26±1	28±1
SAP, mmHg	91±4*	105±4	96±5
DAP, mmHg	62±3	68±4	63±4
MAP, mmHg	72±4	80±4	74±4
PP, mmHg	29±2*	36±2	33±2
Heart rate, bpm	353±30	367±13	315±21
Parameters at 80 mmHg			
Diameter, mm	0.46±0.01	0.47±0.02	0.47±0.02
Distensibility, 10 ⁻³ mmHg ⁻¹	10.0±0.8*	14.0±1.2	12.6±1.0
Comparison within the 72–92 mmHg section of AP			
AUC diameter, mmHg mm	9.2±0.2	9.5±0.3	9.4±0.5
AUC distensibility, 10 ⁻³	192±15*	265±21	241±17
Mean shift of distensibility, Des $-/-$ vs. Des $+/+$, 10 ⁻³ mmHg ⁻¹			
			3.7

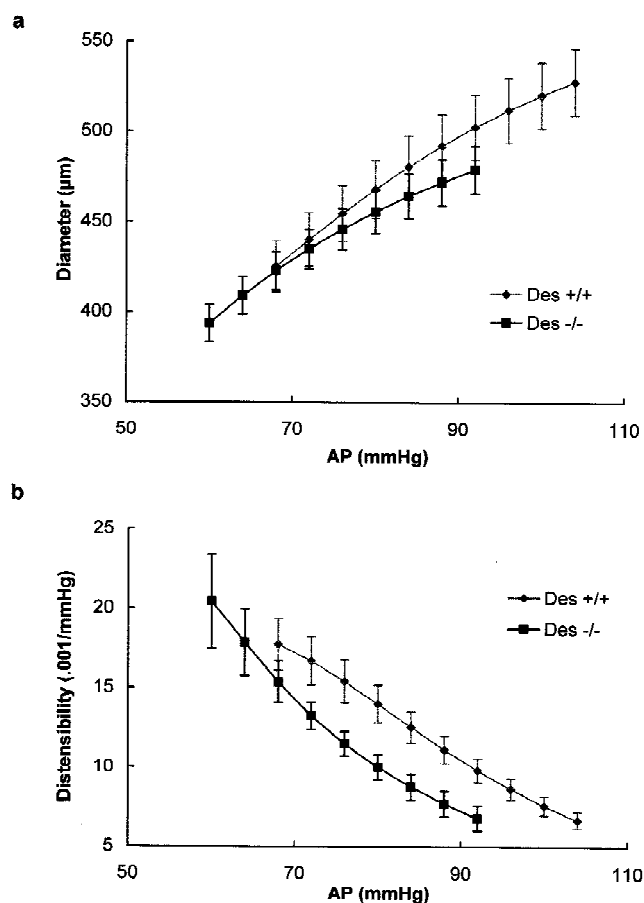
^a Values are mean±S.E.M. **P*<0.05 vs. Des $+/+$.

Fig. 1. In vivo mean carotid diameter–*P* curves (a) and cross-sectional distensibility–*P* curves (b) in 3-month-old Des $-/-$ and Des $+/+$ mice. At a given level of AP, diameter remained unchanged in Des $-/-$. Distensibility–*P* curve of Des $-/-$ was significantly shifted downward compared with Des $+/+$.

Table 2

Viscous parameters of carotid artery studied in vivo in Des $-/-$ mice and Des $+/+$ mice^a

Parameters	Des $-/-$ (n=9)	Des $+/+$ (n=8)
WT, mJ m ⁻¹	0.53±0.06	0.56±0.05
WV, µJ m ⁻¹	29±3*	16±4
WP, % of WT	5.5±0.4*	2.8±0.6

^a WT and WV represent total and viscous energy exchanged from the blood to the arterial wall, respectively. WP represents viscous energy expressed as percent of the total energy. Values are mean±S.E.M. **P*<0.05 vs. Des $+/+$.

Des $-/-$ and Des $+/+$. Fig. 2 illustrates that the hysteresis loop of the diameter–AP curve was higher in Des $-/-$ than in Des $+/+$. The viscous energy (expressed either in absolute values or as percent of the total energy) was twofold higher in Des $-/-$ than in Des $+/+$.

3.2. Desmin expression and SMC proteins

An amplified 353 bp desmin fragment was obtained from carotid arteries and aorta RNA of Des $+/+$ mice whereas this fragment was absent in Des $-/-$, showing the absence of desmin mRNA in Des $-/-$ mice (Fig. 3E). As a control, a 157-bp vimentin fragment was found both in the control and Des $-/-$ mice RNA.

Fig. 3 shows immunohistochemistry analysis, using desmin antibody in cryosections of thoracic aorta (Fig. 3A and B) and carotid artery (Fig. 3C and D). In Des $+/+$, the SMC of the thoracic aorta (Fig. 3A) and carotid artery (Fig. 3C) showed a clear positive immunoreactivity for desmin whereas the SMC of Des $-/-$ (Fig. 3B and D) were completely devoid of desmin positive staining.

Western Blot analysis of SM-MHC SM1 and SM2,

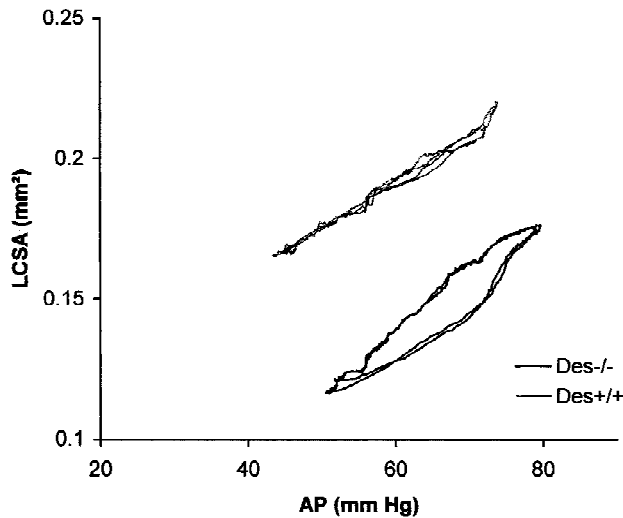


Fig. 2. Typical in vivo tracings of carotid pressure–LCSA curve in one Des $-/-$ and one Des $+/+$ mice. The hysteresis loop area was higher in Des $-/-$ than in Des $+/+$.

NM-MHC, α -actinin, vinculin, and FAK shows no difference of these proteins between Des $-/-$ and Des $+/+$ (data not shown).

3.3. Composition of the carotid artery

Fig. 4 and Table 3 show that arterial thickness and MCSA of in situ fixed vessels were not different between Des $-/-$ and Des $+/+$. Relative and total contents of collagen and elastin as well as the number of nuclei of SMC were similar in Des $-/-$ and Des $+/+$.

3.4. Electron microscopy

In Des $+/+$, the SMC displayed fingerlike projections to anchor them to the elastic lamellae (Fig. 5). In Des $-/-$, the perimeter of cellular fingerlike projections, measured at equivalent mean cellular perimeter, was significantly smaller than in Des $+/+$ mice (146 ± 10 vs. 224 ± 32 μm , $P < 0.05$), indicating that the cells have lost part of their connections to the extracellular matrix (ECM) proteins. The perimeter was not significantly different in Des $+/-$ (183 ± 20 μm) compared to Des $+/+$.

The dense bodies in finger-like projections were present both in Des $-/-$ and Des $+/+$ mice. However, in all observation areas of Des $-/-$, the number of dense bands seemed to decrease and the morphological cell environment appeared very different: in Des $+/+$, the areas between elastic fibers, SMC and basal lamina were thicker

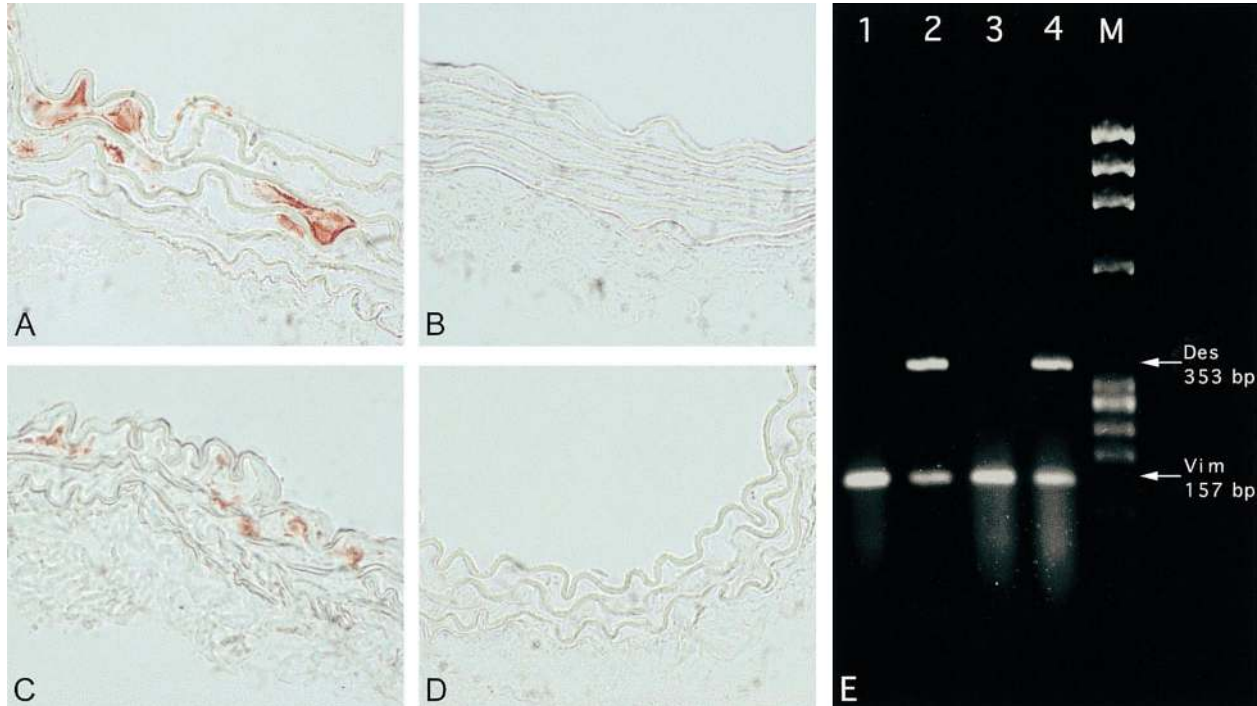


Fig. 3. Desmin immunostaining and desmin–vimentin RT-PCR: immunostaining of thoracic aorta (A, B) and carotid artery (C, D) for desmin in Des $-/-$ (B, D) and Des $+/+$ (A, C) mice; RT-PCR (E), lanes 1–2 with carotid arteries RNA, lanes 3–4 RT-PCR with aortas RNA. A positive desmin immunoreactivity is seen in both the smooth muscle of the carotid artery and the thoracic aorta from Des $+/+$. Desmin staining is completely absent in Des $-/-$. In RT-PCR, an amplified 353 bp desmin fragment indicated by *Des* was obtained from carotid arteries and aorta RNA of control mice (lanes 2 and 4) but absent in the Des $-/-$ mice (lanes 1 and 3). A 157 bp vimentin fragment indicated by *Vim* was found both in the control and desmin knock-out mice RNA. M, DNA marker (Φ X174 digested with *Hae*III).

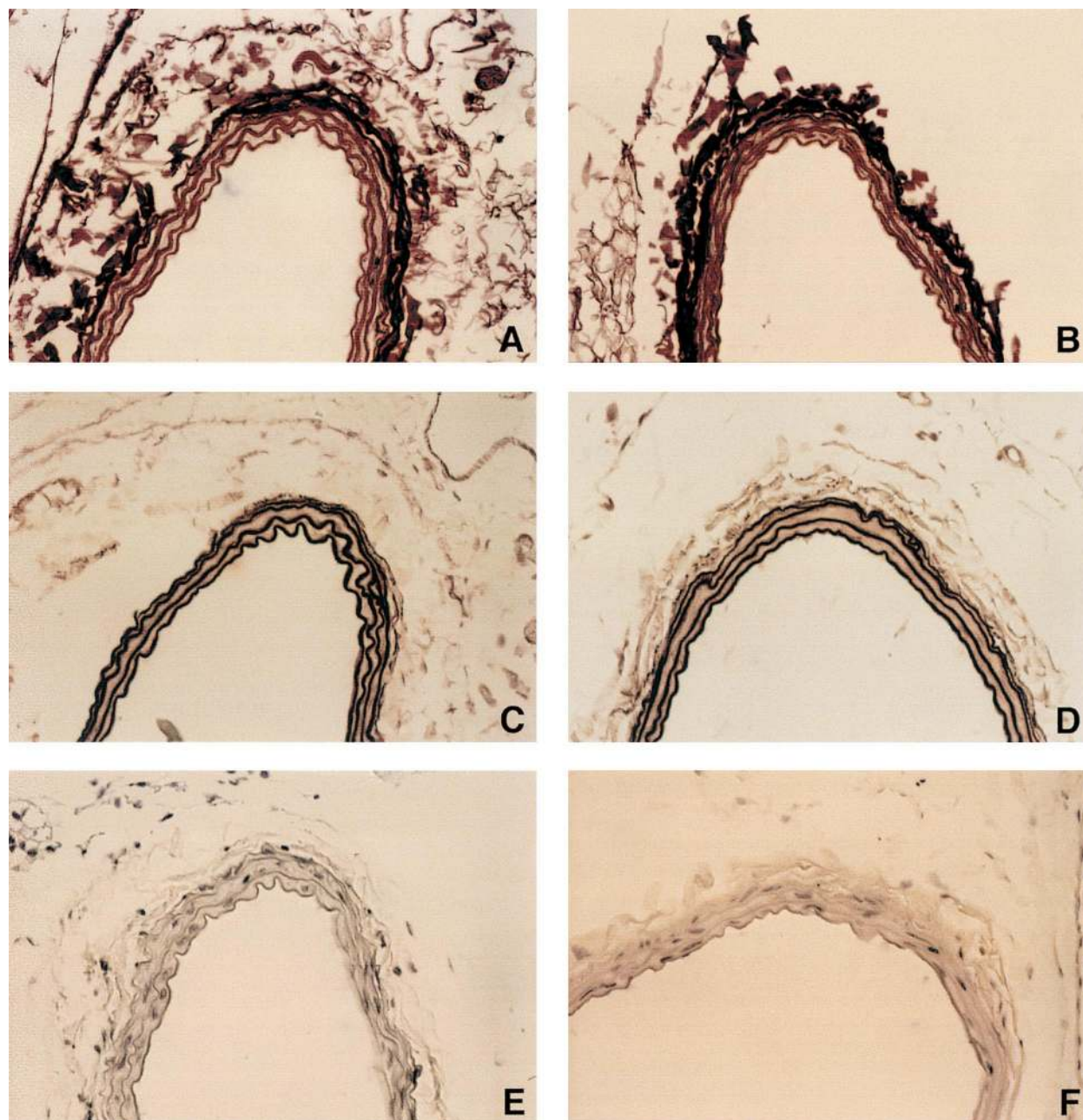


Fig. 4. Structure of the carotid artery in mice lacking desmin: transverse carotid sections of 3-month-old Des +/+ (A, C, E) and Des -/- (B, D, F) stained with sirius red for collagen (A, B), orcein for elastin (C,D), and hematoxylin (E, F) for nucleus staining. The vessels were fixed at physiological pressure with formaldehyde before sectioning. The carotid artery of Des -/- mouse has apparently normal architecture. Collagen and elastin fibers as well as the number of nuclei of smooth muscle cells are preserved. Note similar thickness of the vascular wall in both strains. Objective magnification $\times 40$.

containing more rich and dense materials, such as proteoglycans and collagen fibers. Des -/- mice contained less of these structures suggesting that attachments between cells and matrix are different.

Compared with Des +/+, the SMC of Des -/- showed a very clear cytoplasm: the mitochondria have lost part of their normal organization in packed strands and appeared more scattered.

3.5. Mechanical strength

The CCA which have been freeze dried and directly embedded in paraffin without fixation showed numerous damages of the vascular wall and disorganization of tissue between elastic lamellae in Des -/- (Fig. 6A).

The evolution of the diameter when the in vitro intraluminal pressure was increased was similar in all

Table 3
Histology of the carotid artery in Des $-/-$ mice and Des $+/+$ mice^a

Component/parameter	Des $-/-$ (n=6)	Des $+/+$ (n=6)
Media thickness, μm	16.7 \pm 1.3	16.6 \pm 1.3
MCSA, 10^{-3} mm^2	19 \pm 2	20 \pm 2
Elastin density, %	27.7 \pm 0.9	28.5 \pm 1.8
Elastin content per section, 10^{-3} mm^2	5.4 \pm 0.6	5.7 \pm 0.7
Collagen density, %	21.0 \pm 2.4	23.8 \pm 1.5
Collagen content per section, 10^{-3} mm^2	4.0 \pm 0.5	4.8 \pm 0.8
Nuclei density (normalized per field)	82 \pm 6	83 \pm 3

^a Values are mean \pm S.E.M.

substrains (data not shown). The rupture pressure was significantly lower in Des $-/-$ (1500 \pm 200 mmHg) compared with Des $+/+$ (2100 \pm 80 mmHg, $P < 0.05$, Fig. 6C) indicating a reduction of the mechanical strength of the arterial wall in Des $-/-$. The rupture pressure was not different in Des $+/-$ (2080 \pm 80 mmHg) compared to Des $+/+$.

4. Discussion

We present the first approach of the functional role of desmin in the arterial wall in association with a structural

approach. In the present study, we determined viscoelastic properties, composition and mechanical strength of the carotid artery in transgenic desmin KO mice. The main finding is the loss of mechanical resistance of the vascular wall in Des $-/-$.

In smooth muscle, desmin is associated with Z-disc-like structures called dense bodies. Immunohistochemical staining for desmin is located at the periphery of dense bodies [6]. Intermediate filaments are also found penetrating into some of the membrane-associated dense bands [7,8,22]. The insertion of actin filaments both into the dense bodies and dense bands is well established. Electron microscopy has shown that the dense bands play a major role in regulating contractile and elastic tension in the mouse aorta [23]. However the influence of desmin on membrane-ECM organization is yet unknown. Several authors suggested that desmin filaments link dense bodies together and to the membrane dense bands and thus, might stabilize the contractile units [9,10].

Although the function of desmin remains elusive, studies [24,25] have suggested two hypotheses on the role of desmin in smooth muscle: a function of transcytoplasmic integrating matrix protein supporting cell architecture and/or a function of signal transduction. Desmin can serve as sites of attachment as well as major substrates of several

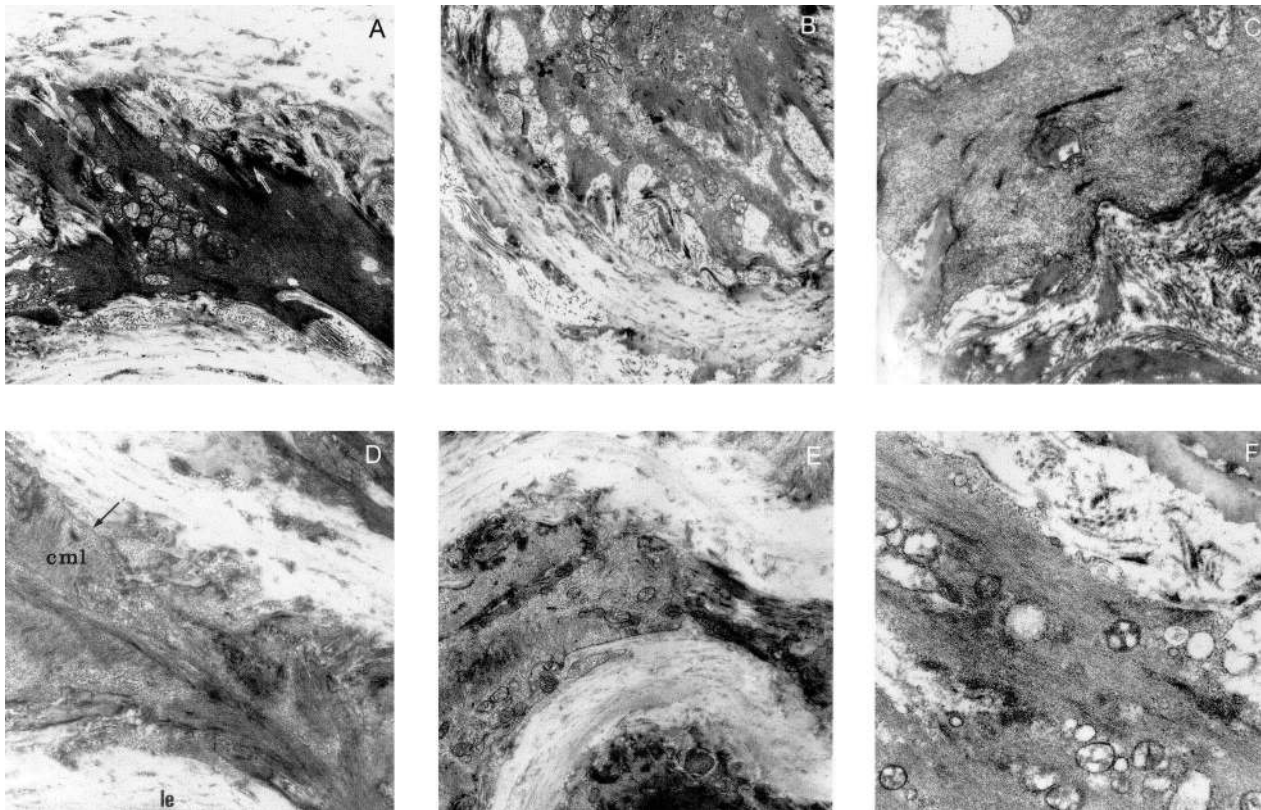


Fig. 5. Transmission electron microscopy of the thoracic aorta from Des $+/+$ (A, B), Des $+/-$ (C), Des $-/-$ (D, E, F) mice: smooth muscle cells (smc) of Des $-/-$ have lost their fingerlike projections (arrows) toward the elastic lamellae (el). Compared with Des $+/+$ and Des $+/-$ mice, the cytoplasm around nuclei appear also very clear with disorganization of mitochondrias. Objective magnification $\times 10\,000$.

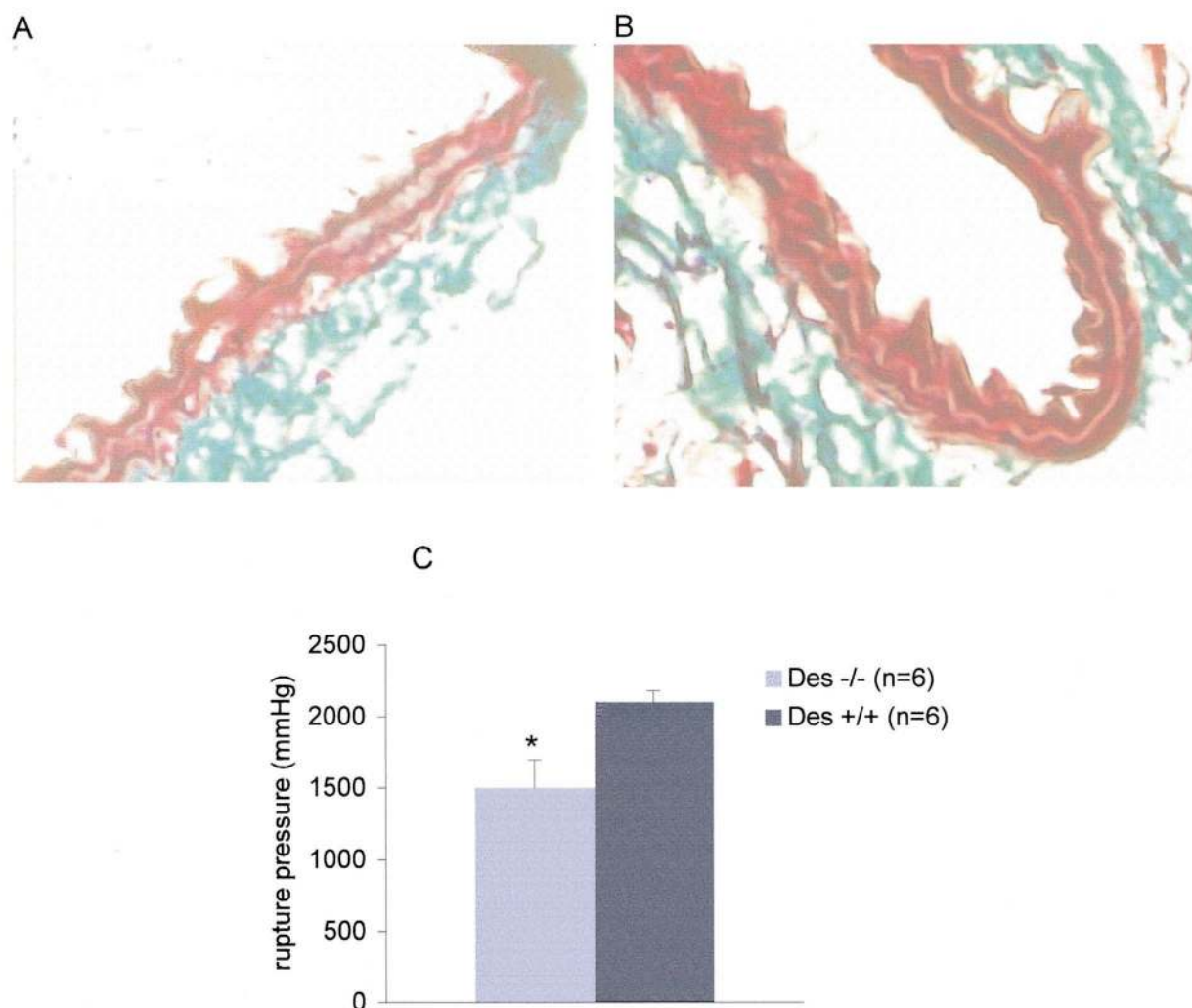


Fig. 6. Excessive fragility of the carotid artery in Des $-/-$: unfixed freeze-dried sections of 3-month-old Des $-/-$ (A) and Des $+/+$ (B) mice stained with orcein and hematoxylin. Objective magnification $\times 100$. Mean arterial in vitro rupture pressure values (C). The rupture pressure is significantly lower in Des $-/-$, $*P < 0.05$.

kinases that seem to be involved in transduction mechanisms.

Recent studies on desmin KO mice have demonstrated [2–5,11] that the three types of muscles have shown severe abnormalities including losses of integrity of myofibrils and tissue cohesion. Whereas desmin is normally expressed together with vimentin in SMC, no overexpression of vimentin compensates for the absence of desmin in Des $-/-$. As far as the arteries of Des $-/-$ are concerned, only the structure of the aorta has been described but there is, to our knowledge, no study of the functional consequences.

Before studying the mechanical properties of the CCA, we have first searched the presence of desmin in the vascular wall of control mice. We showed a positive staining for desmin both in the CCA and thoracic aorta in Des $+/+$ mouse. As previously described in various other mammals [26], vascular SMC appeared to contain only a small amount of desmin. The presence of desmin was

confirmed by RT-PCR analysis showing desmin mRNAs in WT mice. Desmin staining and mRNAs were completely absent in Des $-/-$. We verified that vimentin mRNAs were present both in Des $+/+$ and Des $-/-$ mice. We have studied by Western blot analysis the myosin isoforms and some proteins associated with dense bands. No overexpression of any of these proteins has been detected.

We used high resolution echotracking system to establish the in vivo diameter–AP and distensibility–AP curves. To our knowledge, this is the first time that this echotracking method, already validated in rats [12,13,15,27], was applied to mice. In Des $-/-$, we observed in vivo functional changes, i.e. a lower distensibility and a greater wall viscosity than in Des $+/+$.

Arteries are not purely elastic but exhibit a markedly viscous behavior represented by the hysteresis loop of the pressure–diameter curve. The determinants of AWV are the amplitude and frequency of pulsatile stress and the cytoskeleton of SMC [28–30]. We have previously demon-

strated that AWV is very low in vivo compared with in vitro conditions indicating an active compensatory mechanism [18]. In the present study, we show that the viscosity measured in vivo was twofold higher in Des $-/-$ than in Des $+/+$. Since systolic and pulsatile arterial pressures are slightly reduced in Des $-/-$, the increase in AWV is more likely related to changes in SMC cytoskeleton.

The in vivo arterial distensibility, determined for the common range of blood pressure, was significantly lower in Des $-/-$ compared with Des $+/+$. Neither the composition of the vascular wall, nor the arterial geometry can explain the increase in arterial stiffness since they remained unchanged in Des $-/-$. A possible explanation could be that some modifications in the structural organization of the vascular wall occurred. The classical theory is that the components are arranged in parallel in such a way that circumferential stress is transferred from distensible components (elastin fibers and muscle) to rigid collagen fibers as the vessel is distended further [28]. Smooth muscle and elastin bear most of the stress when the diameter is small. We showed that Des $-/-$ and Des $+/+$ operate at equivalent arterial diameter. Since desmin filaments appear to serve as a scaffolding in SMC for the link of dense bodies to each other and to the membrane associated dense bands, desmin may distribute mechanical forces across the vascular wall [24,25]. The cellular disorganization induced by the lack of desmin may thus transfer the mechanical load from distensible components to stiffer collagen fibers at a lower level of arterial pressure.

Our study was not designed to provide information on the consequences of the lack of desmin on mechanotransduction induced by shear stress. Vimentin is the intermediate filament known to be implicated in this mechanotransduction. Indeed, in mice lacking vimentin, the flow-induced dilation was reduced [31]. In our study, the changes observed in the hemodynamic state may have modified the effects of the shear stress. They could be reinforced by two factors that tend to increase the blood velocity for a given blood flow leading to an increase of the shear stress: the reduction of the mean diameter, and the reduction of distensibility which leads to a reduction of the LCSA expansion during cardiac cycle. The effects of shear stress could be reduced by: the reduction of the pulse pressure known as a determinant of endothelial mechanotransduction, and the possible reduction in cardiac output due to the cardiopathy. However it remains to determine whether desmin may directly influence the mechanotransduction induced by shear stress.

Few studies have previously reported histological analysis of the vascular wall in mice lacking desmin [2,3,10]. They have been performed in the thoracic aorta and after in vitro fixation of the vessel. They described SMC disorganization, hypoplasia, empty space around the nuclei [3] and a reduction of the distance between the elastic layers (due to the loss of SMC) [2]. When the vessel was

fixed in situ at physiological pressure, we observed that there was no evidence for gross macroscopic modifications of the carotid artery in Des $-/-$: elastic lamellae were regularly arranged and there was neither hypoplasia nor reduction of wall thickness. By contrast, arteries which have been first removed and then cryodessicated without fixation, showed disorganization of the vascular wall, thus very similar to those previously reported [3]. One explanation for these discrepancies is that arteries were in a different mechanical state during the fixation procedure. Indeed, when the artery is first removed, then placed in zero pressure condition before fixation [2,3,10], the vessel undergoes significant geometrical modifications, mainly a longitudinal retraction of about 30% and an increase in wall thickness. Before the process of cryodessication, the arterial segments were isolated at zero pressure without fixation and shortened in the same way. In these conditions, the freeze-drying procedure has also produced important damaging of the arterial tissue in Des $-/-$, suggesting an excessive fragility.

As previously described [10], the electron microscopy analysis showed structural modifications of the vascular wall. In the aorta of Des $-/-$, we observed a severe SMC disorganization, a clearing of the cytoplasm around the nuclei and a loss of fingerlike projections toward the elastic lamellae. This result indicates that the absence of desmin was associated with abnormal cell–matrix interactions. This is in accordance with previous studies [3,5] showing a lower tissue cohesion compatible with a higher fragility of the vascular wall.

The measurement of rupture pressure of the vascular wall was used as a quantification of mechanical strength of arteries and it was far from physiologic blood pressure levels. The loss of mechanical resistance of the vascular wall in Des $-/-$ was demonstrated by the results of the in vitro study that showed a reduction of the mechanical strength. The intraluminal pressure inducing the rupture of the vascular was significantly reduced (-29%) in Des $-/-$ compared with Des $+/+$. The comparison between heterozygous mice (Des $+/-$) with wild type (Des $+/+$) showed no significant difference for the rupture pressure neither for the other haemodynamic and mechanical parameters measured.

This finding represents the first demonstration of an excessive fragility of the vascular wall in Des $-/-$. Muscular tissue fragility induced by the lack of desmin has been already described in other tissues [3,5,32], but never to our knowledge in the vascular wall. This excessive fragility of the vascular wall may contribute to aggravate the effects of aging on vascular structure. The reduction of BP observed in vivo may reduce the mechanical solicitation of the arterial wall. Therefore, this can be interpreted as a compensatory mechanism adapted to the excessive fragility of the wall.

In conclusion, although desmin is not absolutely necessary for SMC structure compatible with animal life, it is

essential to maintain proper viscoelastic properties and mechanical strength of the vascular wall. Our results support the hypothesis [4,24] that desmin plays an important role in cell–matrix interactions by its anchorage points with dense bodies and membrane-associated dense bands.

Acknowledgements

This work was supported by INSERM (494014), Fondation de France (96001918) and Ministère de l'Éducation Nationale de la Recherche et de la Technologie (grant ACCSU). We thank Professor Jacques Bonnet for his great support and advice, Mathias Titeux for his help in photographic work, and Claudine Perret for her excellent technical assistance.

References

- [1] Fuchs E, Weber K. Intermediate filaments: structure, dynamics, function, and disease. *Annu Rev Biochem* 1994;63:345–382.
- [2] Li Z, Colucci-Guyon E, Pincon-Raymond M et al. Cardiovascular lesions and skeletal myopathy in mice lacking desmin. *Dev Biol* 1996;175:362–366.
- [3] Milner D, Weitzer G, Tran D, Bradley A, Capetanaki Y. Disruption of muscle architecture and myocardial degeneration in mice lacking desmin. *J Cell Biol* 1996;134:1255–1270.
- [4] Thornell L, Carlsson L, Li Z, Mericskay M, Paulin D. Null mutation in the desmin gene gives rise to a cardiomyopathy. *J Mol Cell Cardiol* 1997;29:2107–2124.
- [5] Li Z, Mericskay M, Agbulut O et al. Desmin is essential for the tensile strength and integrity of myofibrils but not for myogenic commitment, differentiation, and fusion of skeletal muscle. *J Cell Biol* 1997;139:129–144.
- [6] Small J, Furst D, DeMay J. Localization of filamin in smooth muscle. *J Cell Biol* 1986;102:210–220.
- [7] Small JV, Gimona M. The cytoskeleton of the vertebrate smooth muscle cell. *Acta Physiol Scand* 1998;164:341–348.
- [8] Gabella G. Pharmacology of smooth muscle. In: Szekeres L, Papp J, editors, *Handbook of experimental pharmacology*, Springer-Verlag, 1994, pp. 3–34.
- [9] Cooke P. A filamentous cytoskeleton in vertebrate smooth muscle fibers. *J Cell Biol* 1976;68:539–556.
- [10] Capetanaki Y, Milner DJ. Desmin cytoskeleton in muscle integrity and function. *Subcell Biochem* 1998;31:463–495.
- [11] Sjuve R, Arner A, Li Z et al. Mechanical alterations in smooth muscle from mice lacking desmin. *J Muscle Res Cell Motil* 1998;19:415–429.
- [12] Lacolley P, Glaser E, Challande P et al. Structural changes and in situ aortic pressure–diameter relationship in long-term chemical-sympathectomized rats. *Am J Physiol* 1995;269:H407–416.
- [13] Hayoz D, Rutschmann B, Perret F et al. Conduit artery compliance and distensibility are not necessarily reduced in hypertension. *Hypertension* 1992;20:1–6.
- [14] Bezie Y, Lamaziere JM, Laurent S et al. Fibronectin expression and aortic wall elastic modulus in spontaneously hypertensive rats. *Arterioscler Thromb Vasc Biol* 1998;18:1027–1034.
- [15] Glaser E, Lacolley P, Boutouyrie P et al. Dynamic versus static compliance of the carotid artery in living Wistar–Kyoto rats. *J Vasc Res* 1995;32:254–265.
- [16] Langewouters GJ, Wesseling KH, Goedhard WJ. The static elastic properties of 45 human thoracic and 20 abdominal aortas in vitro and the parameters of a new model. *J Biomech* 1984;17:425–435.
- [17] Boutouyrie P, Bezie Y, Lacolley P et al. In vivo/in vitro comparison of rat abdominal aorta wall viscosity. Influence of endothelial function. *Arterioscler Thromb Vasc Biol* 1997;17:1346–1355.
- [18] Boutouyrie P, Boumaza S, Challande P, Lacolley P, Laurent S. Smooth muscle tone and arterial wall viscosity: an in vivo/in vitro study. *Hypertension* 1998;32(2):360–364.
- [19] Stein H, Gatter K, Asbahr H, Mason DY. Use of freeze-dried paraffin-embedded sections for immunohistologic staining with monoclonal antibodies. *Lab Invest* 1985;52:676–683.
- [20] Louis H, Lavie J, Lacolley P et al. Freeze-drying allows double nonradioactive ISH and antigenic labeling. *J Histochem Cytochem* 2000;48:499–508.
- [21] L'Heureux N, Paquet S, Labbe R, Germain L, Auger FA. A completely biological tissue-engineered human blood vessel. *FASEB J* 1998;12:47–56.
- [22] Bagby RM. Organization of contractile elements. In: Stephens NL, editor, *The biochemistry of smooth muscle*, Boca Raton, FL: CRC Press, 1983, pp. 1–84.
- [23] Davis EC. Smooth muscle cell to elastic lamina connections in developing mouse aorta. Role in aortic medial organization. *Lab Invest* 1993;68:89–99.
- [24] Lazarides E. Intermediate filaments as mechanical integrators of cellular space. *Nature* 1980;283:249–256.
- [25] Wang N, Butler JP, Ingber DE. Mechanotransduction across the cell surface and through the cytoskeleton. *Science* 1993;260:1124–1127.
- [26] Gabbiani G, Schmid E, Winter S et al. Vascular smooth muscle cells differ from other smooth muscle cells: predominance of vimentin filaments and a specific alpha-type actin. *Proc Natl Acad Sci USA* 1981;78:298–302.
- [27] van Gorp A, van Ingen Schenau D, Hoeks A et al. Aortic wall properties in normotensive and hypertensive rats of various ages in vivo. *Hypertension* 1995;26:363–368.
- [28] Milnor W. Properties of the vascular wall. In: Collins N, editor, *Hemodynamics*, Baltimore, MD: Williams and Wilkins, 1989, pp. 58–101.
- [29] Levy B. Mechanics of the large artery vascular wall. In: Levy B, Tedgui A, editors, *Biology of the arterial wall*, Dordrecht: Kluwer Academic, 1999, pp. 13–24.
- [30] Janmey PA. The cytoskeleton and cell signaling: component localization and mechanical coupling. *Physiol Rev* 1998;78:763–781.
- [31] Henrion D, Terzi F, Matrougui K et al. Impaired flow-induced dilation in mesenteric resistance arteries from mice lacking vimentin. *J Clin Invest* 1997;100:2909–2914.
- [32] Fuchs E, Cleveland DW. A structural scaffolding of intermediate filaments in health and disease. *Science* 1998;279:514–519.